Magneto-Coulomb Drag and Hall Drag in Double-Layer Dirac Systems

Wang-Kong Tse,[1] Ben Yu-Kuang Hu,[2] J. N. Hong,[1] and A. H. MacDonald[3]
[1]Department of Physics and Astronomy, Center for Materials for Information Technology, The University of Alabama, Alabama 35487, USA
[2]Department of Physics, The University of Akron, Akron, Ohio 44325, USA
[3]Department of Physics, University of Texas, Austin, Texas 78712, USA

(Received 17 November 2017; revised manuscript received 3 August 2018; published 10 May 2019)

We develop a theory of Coulomb drag due to momentum transfer between graphene layers in a strong magnetic field. The theory is intended to apply in systems with disorder that is weak compared to Landau level separation, so that Landau level mixing is weak but strong compared to correlation energies within a single Landau level, so that fractional quantum Hall physics is not relevant. We find that, in contrast to the zero-field limit, the longitudinal magneto-Coulomb drag is finite and, in fact, attains a maximum at the simultaneous charge neutrality point (CNP) of both layers. Our theory also predicts a sizable Hall drag resistivity at densities away from the CNP.

DOI: 10.1103/PhysRevLett.122.186602

Introduction.—Progress in preparing high-quality samples of graphene [1,2] and other atomically thin two-dimensional (2D) systems has made it possible to study interlayer interaction effects in Coulomb-coupled electron gas layers separated by only a few nanometers. The archetypical Coulomb-coupling phenomenon is drag resistance due to Coulomb interactions between layers [3]. When an external electric field drives a current through one of the layers, there is a nonzero rate of net momentum transfer from electrons in the drive layer to electrons in the drag layer, resulting in a *drag voltage* in an open-circuit geometry. This intriguing effect has been extensively studied theoretically and experimentally in conventional 2D electron gas (2DEG) systems. Atomically thin Dirac electron systems like graphene present new challenges to theories of Coulomb drag, because stronger coupling can be achieved by placing the two layers closer together [4,5].

The weak coupling regime of Coulomb drag in a double-layer graphene system has been explored theoretically [6–14] and realized experimentally [15]. Striking differences compared with the zero-field case are observed [16–19] when closely separated ($\gtrsim$1 nm) double-layer graphene or bilayer graphene structures are placed in weak perpendicular magnetic fields. The observations of a finite longitudinal drag resistivity at the simultaneous charge neutrality point (CNP) of both layers and of a large Hall drag away from this density have been particularly intriguing. Very recently, strong-field Coulomb drag in the quantum Hall regime has been measured in double layers of graphene [22] and bilayer graphene [20,21].

In this Letter, we develop a theory of Coulomb drag due to *momentum exchange* between 2D graphene sheets in the presence of strong magnetic fields. We consider the case where fields are strong enough for weakly disorder-broadened Landau levels to be well resolved. Our theory does not apply when an exciton condensate is present or in the weak-disorder, low-temperature regime at which the fractional quantum Hall effect and other phenomena associated with strong electronic correlations appear. We find that the drag resistivity behaves very differently in the strong magnetic field and zero magnetic field limits. As we will show, a finite drag resistivity is present at the simultaneous CNP of both layers at strong fields, whereas drag vanishes at that point in the $B = 0$ case [6]. Away from the CNP, we find a sizable Hall drag resistivity. These two main findings from our theory corroborate recent experimental observations [22].

Theory.—The eigenstates of the graphene free-particle Hamiltonian consist of a special Dirac point Landau level (LL) labeled by $(n = 0, X)$, and other LLs labeled by (n, s, X), where $n = 1, 2, \ldots$ is a LL index, $s = \pm$ is a band label (conduction band $+$ and valence band $-$), and X is a Landau gauge guiding center label. The LL energies are $s\varepsilon_n = s\hbar\omega_c\sqrt{n}$, where $\omega_c = \sqrt{2}v/\ell_B$ with v the Dirac velocity ($v = 10^6$ ms^{-1} in graphene) and $\ell_B = \sqrt{\hbar/e|B|}$ the magnetic length [23]. Our theory is applicable in the regime $k_BT,\ \Delta\varepsilon \gg \hbar/\tau$, where $\Delta\varepsilon$ is the typical LL separation near the Fermi level and $\hbar/\tau$ the disorder broadening. The central quantity in the Coulomb drag problem [24,25] is the nonlinear susceptibility $\mathbf{\Gamma}(\mathbf{q}, \omega, \mathbf{B})$ [see Fig. 1(a)]. We now derive an expression for this quantity that is valid for graphene in a magnetic field. The Green's function in Fig. 1(a) is

$$G_{n,s,X}(\varepsilon) = \frac{|n, s, X\rangle\langle n, s, X|}{\varepsilon - \varepsilon_{s,n} + i/2\tau}, \tag{1}$$

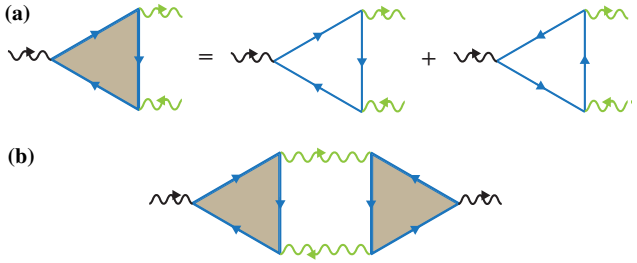

FIG. 1. (a) Diagrams for the nonlinear susceptibility Γ. The black (dark) wavy line denotes a vector potential coupled to a current vertex, and the light (green) wavy lines denote scalar potentials coupled to charge vertices. (b) Diagram for the drag transconductivity. Interlayer screened Coulomb interactions [green (light) wave lines] representing interlayer Coulomb interactions $U(q,\omega)$ link the two triangle nonlinear susceptibility diagrams.

where $|n,s,X\rangle$ is an eigenstate [26]. The three vertices in the nonlinear susceptibility diagram [Fig. 1(a)] contain matrix elements of the current and charge density operators between different LL wave functions. In a continuum model, the eigenstates are spinors with components on both honeycomb sublattices. The current and charge density matrix elements are

$$\langle n_2,s_2,X_2|j_x|n_3,s_3,X_3\rangle = ev\delta_{X_2,X_3}\mathcal{N}_{n_2}\mathcal{N}_{n_3} \times [s_2\delta_{n_2-1,n_3}+s_3\delta_{n_2,n_3-1}], \quad (2)$$

$$\langle n_1,s_1,X_1|e^{i\mathbf{q}\cdot\mathbf{r}}|n_2,s_2,X_2\rangle = \delta_{X_1,X_2+q_y\ell_B^2}e^{iq_x(X_1+X_2)/2}\mathcal{N}_{n_1}\mathcal{N}_{n_2} \times [F_{n_1,n_2}(\mathbf{q})+s_1s_2F_{n_1-1,n_2-1}(\mathbf{q})], \quad (3)$$

where $\mathcal{N}_n=\delta_{n,0}+(1-\delta_{n,0})/\sqrt{2}$ is a normalization factor, and we have defined

$$F_{n_1,n_2}(\mathbf{q}) = \sqrt{\frac{n_<!}{n_>!}}e^{-q^2\ell_B^2/4}L_{n_<}^{n_>-n_<}\left(\frac{q^2\ell_B^2}{2}\right)\left(\frac{i\tilde{q}\ell_B}{\sqrt{2}}\right)^{n_>-n_<}. \quad (4)$$

In Eq. (3), $q=|\mathbf{q}|$, $\tilde{q}=q_x+iq_y$, $n_>=\max(n_1,n_2)$, $n_<=\min(n_1,n_2)$, and L_n^α is the generalized Laguerre polynomial of degree n. Evaluating Fig. 1(a) using the standard Matsubara Feynman diagram technique and Eqs. (1)–(4), we obtain the following compact expression for the nonlinear susceptibility:

$$\mathbf{\Gamma}(\mathbf{q},\omega,\mathbf{B}) = 2\ell_B^2\mathbf{q}\times\hat{\mathbf{B}}\mathrm{Im}\Pi(q,\omega,B), \quad (5)$$

where $\hat{\mathbf{B}}$ is the direction of the magnetic field,

$$\Pi(q,\omega,B) = -\frac{g}{2\pi\ell_B^2}\sum_{n_1,n_2=0}^{\infty}\sum_{s_1,s_2=\pm} \times\frac{f_{s_1,n_1}-f_{s_2,n_2}}{\omega+s_1\varepsilon_{n_1}-s_2\varepsilon_{n_2}+i/2\tau} \times\mathcal{F}_{s_1,s_2}(q\ell_B,n_1,n_2), \quad (6)$$

where $g=4$ accounts for the spin and valley degeneracy and $f_{s,n}$ is the Fermi occupation factor for the (n,s,X) LL. The form factor $\mathcal{F}$ in Eq. (6) is

$$\mathcal{F}_{s_1,s_2}(x,n_1,n_2) = \frac{e^{-x^2/2}}{4}\left(\frac{x^2}{2}\right)^{n_>-n_<} \times\left[s_1\sqrt{\frac{n_<!}{n_>!}}L_{n_<}^{n_>-n_<}\left(\frac{x^2}{2}\right) +s_2\sqrt{\frac{(n_<-1)!}{(n_>-1)!}}L_{n_<-1}^{n_>-n_<}\left(\frac{x^2}{2}\right)\theta(n_<-1)\right]^2, \quad (7)$$

where $\theta(x)=1$ for $x\geq 0$ and 0 otherwise. The quantity Π in Eq. (6) is the polarization function of Dirac fermions in a perpendicular quantizing magnetic field [27]. The nonlinear susceptibility $\mathbf{\Gamma}$ is therefore directly proportional to the imaginary part of the polarization function, as in the conventional 2DEG case with a single *nonchiral* parabolic band [28].

This finding might seem surprising, since the $\Gamma(q,\omega)\propto\mathrm{Im}\Pi(q,\omega)$ property of a conventional 2DEG [24,25] does not apply to the nonlinear susceptibility of graphene [7] in the absence of a magnetic field. This difference can be explained by noting that, while the energy dispersions of the conventional 2DEG and graphene are different at $B=0$, both have dispersionless Landau levels at strong B. We therefore conjecture that, in a strong magnetic field when disorder does not appreciably mix Landau levels, the simple relationship $\Gamma\propto\mathrm{Im}\Pi(q,\omega)$ is a universal feature of *all* clean two-dimensional electron systems, regardless of their energy dispersions. In such a case, the nonlinear susceptibility is, like the polarization function, dominated by inelastic inter-LL transitions of electrons from one localized LL orbit to another localized LL orbit.

Another remarkable distinction of the strong magnetic field is brought to light by examining the drag resistivity at the CNP. The nonlinear susceptibility of graphene in the absence of a magnetic field was first evaluated in Ref. [6]. Making use of the electron-hole symmetry of the bands and time-reversal invariance, it is straightforward to show that, at $B=0$, $\mathbf{\Gamma}(q,\omega)$ is an odd function of the chemical potential μ. When the chemical potential is at the Dirac point, $\Gamma=0$, because the two diagrams comprising Fig. 1(a) exactly cancel. Drag therefore vanishes when either layer is charge neutral. At high temperatures, this behavior has indeed been observed experimentally [15,16]. In the presence of a strong

magnetic field, on the other hand, the nonlinear susceptibility Eq. (5) is an *even* function of μ, as we prove below.

First, we note that electron-hole symmetry is preserved for the $s = \pm$LLs so that $f_{s,n}(\mu) = 1 - f_{-s,n}(-\mu)$ and that the form factor in Eq. (7) is invariant under $s_1 \to -s_1$ and $s_2 \to -s_2$. Next, we can interchange the labels $n_1 \leftrightarrow n_2$, $s_1 \leftrightarrow s_2$ to conclude that $\Pi(q, \omega, B)$ is invariant under $\mu \to -\mu$. It then follows from Eq. (5) that $\mathbf{\Gamma}(\mathbf{q}, \omega, \mathbf{B}; \mu) = -\mathbf{\Gamma}(-\mathbf{q}, \omega, \mathbf{B}; -\mu) = \mathbf{\Gamma}(\mathbf{q}, \omega, \mathbf{B}; -\mu)$. The final identity requires the observation that the form factors in Eq. (7) depend on $q = |\mathbf{q}|$ only. Therefore, the contributions from the two diagrams in Fig. 1(a) do not cancel at $\mu = 0$ as they do in the absence of broken time-reversal symmetry. Drag can be finite even when one of the layers is charge neutral.

The interlayer transconductivity diagrams [24,25] yield the drag conductivity [Fig. 1(b)]

$$\sigma^D_{\alpha\beta} = \frac{e^2}{16\pi\hbar k_B T} \sum_q \int_{-\infty}^{+\infty} \frac{d\omega}{\sinh^2(\omega/2k_BT)} \times \Gamma^L_\alpha(\mathbf{q}, \omega, \mathbf{B}) \Gamma^R_\beta(\mathbf{q}, \omega, -\mathbf{B}) |U(q, \omega, B)|^2, \quad (8)$$

where the superscripts "L" and "R" (left and right, respectively) label the two layers and $U(q, \omega, B)$ is the screened interlayer Coulomb interaction in the random phase approximation [29]. The Coulomb interaction strength in graphene is characterized by the dimensionless coupling constant $\alpha_G = e^2/(\epsilon\hbar v)$, where ϵ is an effective dielectric constant which we view as a parameter that can be altered by changing the sheet's dielectric environment [30]. The quantity measured in most Coulomb drag experiments is the drag resistivity, which can be obtained by inverting the four-component (two layers each with two directions) conductivity tensor $\overleftrightarrow{\sigma}$ of the bilayer, $\overleftrightarrow{\rho} = (\overleftrightarrow{\sigma})^{-1}$. The conductivity tensor becomes diagonal in Cartesian labels when $\hat{\mathbf{x}}$ and $\hat{\mathbf{y}}$ components are replaced by left- and right-handed ($\hat{x} \pm i\hat{y}$) components. It simplifies further in the special case of identical left and right sheets, since parallel flow and counterflow are then decoupled.

For the general case, we introduce the definitions

$$\mathcal{S}_{xx} = (\sigma^D_{xx})^2 - \sigma^L_{xx}\sigma^R_{xx} + \sigma^L_{xy}\sigma^R_{xy}, \quad (9)$$

$$\mathcal{S}_{xy} = \sigma^L_{xy}\sigma^R_{xx} + \sigma^L_{xx}\sigma^R_{xy}, \quad (10)$$

where $\sigma^{L,R}_{xx}$ and $\sigma^{L,R}_{xy}$ are the longitudinal and Hall conductivities, respectively, in the individual layers. Because the Hall drag conductivity σ^D_{xy} vanishes due to the odd momentum dependence of $\mathbf{\Gamma} \propto \mathbf{q} \times \hat{\mathbf{B}}$ in Eq. (5), the general drag resistivity tensor expression simplifies to

$$\rho^D_{\alpha\beta} = \sigma^D_{xx}\mathcal{S}_{\alpha\beta}/(\mathcal{S}^2_{xx} + \mathcal{S}^2_{xy}), \quad (11)$$

where $\alpha, \beta = x$ or y. In 2DEG systems, the Hall drag resistivity is negligible for $\omega_c\tau \ll 1$, where ω_c is the cyclotron frequency [24,33]. In strong magnetic fields, the Hall drag resistivity is finite and can be significant, arising from the longitudinal drag combined with the intralayer Hall responses $\sigma^{L,R}_{xy}$ [34]. From Eq. (10), we observe that the Hall drag ρ^D_{xy} is comparable to the longitudinal drag ρ^D_{xx} in magnitude except when (i) both layers are characterized by well-formed quantum Hall plateaus such that the longitudinal conductivities vanish $\sigma^{L,R}_{xx} = 0$, or (ii), since $\sigma^{L,R}_{xx}(\mu) = \sigma^{L,R}_{xx}(-\mu)$ and $\sigma^{L,R}_{xy}(\mu) = -\sigma^{L,R}_{xy}(-\mu)$, the two layers have opposite carrier densities [15–17].

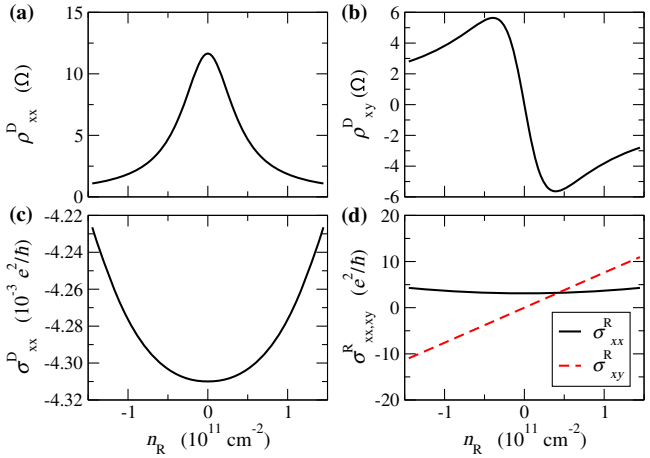

FIG. 2. Longitudinal (a) and Hall (b) drag resistivities of double-layer graphene as a function of right-layer electron density n_R for $n_L = 0$, $B = 0.5$ T, $T = 300$ K, $d = 30$ Å, $1/2\tau = 1$ meV, and $\alpha_G = 0.4$. The filling factor is $\nu = 4.143n[10^{11}\ \text{cm}^{-2}]/B[T] \approx \pm 12$ for this range of density. (c) shows the corresponding drag conductivities and (d) the longitudinal and Hall conductivities.

Dirac-point drag and Hall drag.—In the following, we present numerical results for the drag resistivities evaluated from Eqs. (8)–(11). We employ the Thomas-Fermi approximation in the screened interlayer Coulomb interaction [30]. We first keep the density of one layer (n_L) fixed at the CNP and vary the density of the other layer (n_R). Figure 2(a) shows the longitudinal drag resistivity as a function of the density in the vicinity of the CNP for $B = 0.5$ T. The most important feature we find is that ρ^D_{xx} has its maximum value at the simultaneous CNP $n_{L,R} = 0$. Away from the CNP, ρ^D_{xx} is an even function of n_R and decreases with its magnitude. In Fig. 2(b), we show the Hall drag resistivity ρ^D_{xy}, which is an odd function of n_R. The magnitude of ρ^D_{xy} rises sharply from zero away from the simultaneous CNP and then drops gradually as the layer's carrier density is further increased. In Figs. 2(c) and 2(d), we also depict the behavior of the drag conductivity as well as the R layer's longitudinal and Hall conductivities. As shown in Fig. 2(c), the magnitude of the drag conductivity $|\sigma^D_{xx}|$ decreases with the density. We note that the sign of the drag conductivity is negative and its value is 3 orders of magnitude smaller than the longitudinal and Hall conductivities $\sigma_{xx,xy}$, which results in a positive

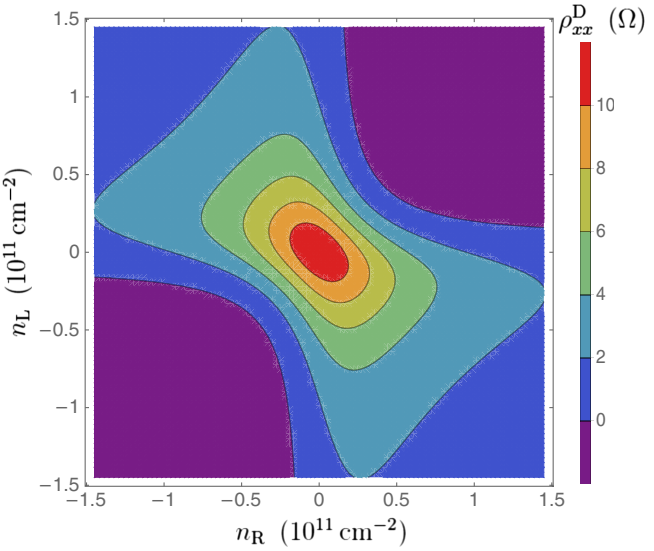

FIG. 3. Longitudinal drag resistivity as a function of right-layer electron density n_R and left-layer electron density n_L for the same values of B, T, d, and α_G as in Fig. 2.

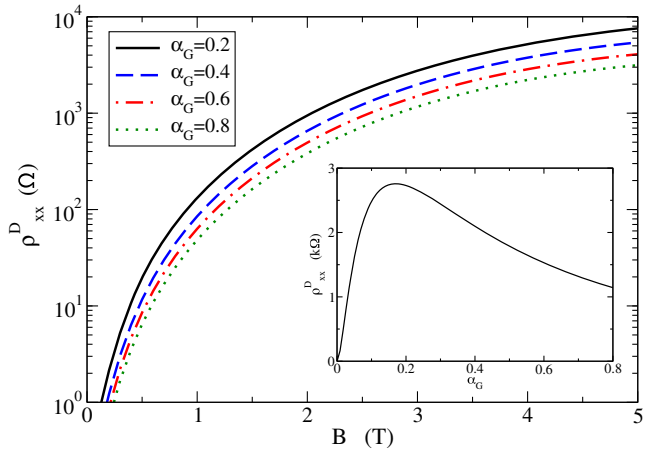

FIG. 4. Longitudinal drag resistivity at the simultaneous CNP $n_L = n_R = 0$ as a function of the magnetic field for different values of interaction coupling $\alpha_G = 0.2, 0.4, 0.6, 0.8$. Inset: The same quantity as a function of α_G at a fixed magnetic field $B = 3$ T. T and d are the same as in previous figures.

sign of the drag resistivity ρ^D_{xx}. Since $\sigma^L_{xy} = 0$ and $\sigma^D_{xx} \ll \sigma^{L,R}_{xx}$, from Eqs. (9)–(11) we observe that the peak of ρ^D_{xy} occurs approximately when $|\sigma^R_{xx}| = |\sigma^R_{xy}|$, which is a consequence of the open-circuit condition of the drag layer.

Figure 3 shows the dependence of ρ^D_{xx} on n_L and n_R. We observe that ρ^D_{xx} is positive in the two quadrants of electron-hole drag, where the L and R carriers have opposite polarities, and mostly negative in the quadrants of electron-electron and hole-hole drag, with $\rho^D_{xx} < 0$ except near the simultaneous CNP at $n_{L,R} \lesssim 10^{10}$ cm^{-2}. These features are in good agreement with the latest experiment [22] performed under strong magnetic fields. With the exception of the CNP vicinity, the signs of magnetodrag for the cases of same and opposite carrier polarities depicted in Fig. 3 are the same as that in the zero-field case [6,7,15,16] and consistent with magnetodrag in conventional 2DEGs [28]. Unlike conventional 2DEGs, however, which would exhibit no drag when the carrier density is tuned to zero in one of the layers, double-layer graphene exhibits a distinctive finite magnetodrag at the simultaneous CNP due to the presence of a Dirac sea of electrons and a gapless energy dispersion. While interlayer energy transfer has been proposed as a possible mechanism [12] to explain the finite negative drag resistivity at the CNP observed in zero-field experiments, we emphasize that such a mechanism does not produce the finite positive drag at the CNP [37] in the presence of a strong magnetic field that is predicted by our theory.

The fact that σ^D_{xx} is nonzero and has a negative sign at $\mu = 0$ can be physically explained as follows. Let us assume that the magnetic field is in the z direction and the electric field is applied to the active layer in the positive y direction. Assuming that the longitudinal components are negligible compared to the transverse components of the intralayer $\sigma^{L,R}$, this implies that particle currents in the active layer are in the positive x direction (independent of whether they are electrons or holes). Therefore, the drag force on the passive layer is in the positive x direction. This acts like an effective electric field in the positive (negative) x direction for holes (electrons), which results in an "$\mathbf{E}$" $\times$ $\mathbf{B}$ drift of the holes (electrons) in the negative (positive) y direction. Hence, for both electrons and holes, the electric current in the passive layer is in the negative y direction; i.e., $\sigma^D_{xx} < 0$. At a finite temperature, the drag currents due to thermally excited electrons and holes reinforce each other and do not cancel. The drag conductivity is an even function of the chemical potential, consistent with the evenness of Γ discussed above.

Since a negative longitudinal conductivity results in a thermodynamic instability, our findings beg an important question: Does a negative drag conductivity also imply a thermodynamic instability? The condition for thermodynamic stability is that the conductivity matrix be positive definite. In the presence of a magnetic field, the Hall conductivities render the conductivity matrix $\overleftrightarrow{\sigma}$ antisymmetric. For an arbitrary square matrix that is not necessarily symmetric, the positive definiteness condition depends on the positivity of the determinant of the symmetric part of the matrix only [36]. It follows that the Hall conductivities $\sigma^{L,R}_{xy}$ drop out, and the resulting determinant is given by $\sigma^L_{xx}\sigma^R_{xx} - (\sigma^D_{xx})^2$, which is positive definite, sharing the same expression with the $B = 0$ case.

Finally, we have calculated the longitudinal drag resistivity ρ^D_{xx} at the simultaneous CNP as a function of the magnetic field for different values of the interaction parameter α_G. Figure 4 shows that ρ^D_{xx} is highly sensitive to changing the magnetic field strength, increasing to several kΩs over a few teslas. It also shows that changing

the electron-electron interaction strength α_G from 0.2 to 0.8 counterintuitively *decreases* ρ_{xx}^D. This finding can be explained by examining the α_G dependence of the interlayer interaction $U(q,\omega,B)$ [30]. Unlike the single-layer case, where the screened interaction $V \sim \alpha_G/(1+\alpha_G)$ monotonically increases with α_G, the screened interlayer interaction of a bilayer $U \sim \alpha_G/(1+\alpha_G^2)$ decreases for large α_G. This behavior is fully reflected in the drag resistivity as a function of α_G depicted in the inset in Fig. 4.

In summary, we find that the magnetodrag resistivity of graphene double layers has a maximum and that the Hall drag resistivity vanishes at the simultaneous CNP. The Hall drag resistivity is, however, comparable to the longitudinal resistivity at nearby densities, even though the Hall drag conductivity vanishes. Our theory accounts for momentum transfer due to interactions between density fluctuations in the two layers but does not account for strong correlations or address all possible scenarios that have been raised [17,38] in connection with graphene double-layer magnetodrag. The physics we explore must, however, contribute significantly to any magnetodrag measurements.

Work at Alabama (W.-K. T. and J. N. H.) was supported by startup and Research Grants Committee funds from the University of Alabama. A. H. M. was supported by the Department of Energy Division of Materials Sciences and Engineering under Grant No. DE-FG02-ER45958 and by the Welch foundation under Grant No. TBF1473. B. Y. K. H. acknowledges support from the University of Akron for a Professional Development Leave.

[1] A. H. C Neto, F. Guinea, N. M. R. Peres, K. S. Novoselov, and A. K. Geim, Rev. Mod. Phys. **81**, 109 (2009).
[2] S. D. Sarma, S. Adam, E. H. Hwang, and E. Rossi, Rev. Mod. Phys. **83**, 407 (2011).
[3] B. N. Narozhny and A. Levchenko, Rev. Mod. Phys. **88**, 025003 (2016).
[4] K. S. Novoselov, A. Mishchenko, A. Carvalho, and A. H. C. Neto, Science **353**, 461 (2016).
[5] A. K. Geim and I. V. Grigorieva, Nature (London) **499**, 419 (2013).
[6] W.-K. Tse, B. Y.-K. Hu, and S. D. Sarma, Phys. Rev. B **76**, 081401(R) (2007).
[7] M. I. Katsnelson, Phys. Rev. B **84**, 041407(R) (2011).
[8] E. H. Hwang, R. Sensarma, and S. D. Sarma, Phys. Rev. B **84**, 245441 (2011).
[9] N. M. R. Peres, J. M. B. L. dos Santos, and A. H. C. Neto, Europhys. Lett. **95**, 18001 (2011).
[10] B. N. Narozhny, M. Titov, I. V. Gornyi, and P. M. Ostrovsky, Phys. Rev. B **85**, 195421 (2012).
[11] M. Carrega, T. Tudorovskiy, A. Principi, M. I. Katsnelson, and M. Polini, New J. Phys. **14**, 063033 (2012).
[12] J. C. W. Song and L. S. Levitov, Phys. Rev. Lett. **109**, 236602 (2012).
[13] J. C. W. Song and L. S. Levitov, Phys. Rev. Lett. **111**, 126601 (2013).
[14] J. C. W. Song, D. A. Abanin, and L. S. Levitov, Nano Lett. **13**, 3631 (2013).
[15] S. Kim, I. Jo, J. Nah, Z. Yao, S. K. Banerjee, and E. Tutuc, Phys. Rev. B **83**, 161401(R) (2011); S. Kim and E. Tutuc, Solid State Commun. **152**, 1283 (2012).
[16] R. V. Gorbachev, A. K. Geim, M. I. Katsnelson, K. S. Novoselov, T. Tudorovskiy, I. V. Grigorieva, A. H. MacDonald, K. Watanabe, T. Taniguchi, and L. A. Ponomarenko, Nat. Phys. **8**, 896 (2012).
[17] M. Titov, R. V. Gorbachev, B. N. Narozhny, T. Tudorovskiy, M. Schutt, P. M. Ostrovsky, I. V. Gornyi, A. D. Mirlin, M. I. Katsnelson, K. S. Novoselov, A. K. Geim, and L. A. Ponomarenko, Phys. Rev. Lett. **111**, 166601 (2013).
[18] J. I. A. Li, T. Taniguchi, K. Watanabe, J. Hone, A. Levchenko, and C. R. Dean, Phys. Rev. Lett. **117**, 046802 (2016).
[19] K. Lee, J. Xue, D. C. Dillen, K. Watanabe, T. Taniguchi, and E. Tutuc, Phys. Rev. Lett. **117**, 046803 (2016).
[20] J. I. A. Li, T. Taniguchi, K. Watanabe, J. Hone, and C. R. Dean, Nat. Phys. **13**, 751 (2017).
[21] X. Liu, K. Watanabe, T. Taniguchi, B. I. Halperin, and P. Kim, Nat. Phys. **13**, 746 (2017).
[22] X. Liu, L. Wang, K. C. Fong, Y. Gao, P. Maher, K. Watanabe, T. Taniguchi, J. Hone, C. Dean, and P. Kim, Phys. Rev. Lett. **119**, 056802 (2017).
[23] Graphene has a g factor of $\sim$2, and the Zeeman energy $g\mu_B B \approx 0.1B$ meV is negligible compared to the typical energy scales for temperature and LL separation considered in this work for B up to $\sim$10 T.
[24] A. Kamenev and Y. Oreg, Phys. Rev. B **52**, 7516 (1995).
[25] K. Flensberg, B. Y.-K. Hu, A.-P. Jauho, and J. M. Kinaret, Phys. Rev. B **52**, 14761 (1995).
[26] For compactness and uniformity, we use the same notation $\varepsilon_{s,n}$ and $|n,s,X\rangle$ for all LLs including $n=0$, with $\varepsilon_{s,n=0} \equiv 0$ and $|n=0,s,X\rangle \equiv |0,X\rangle$.
[27] K. Shizuya, Phys. Rev. B **75**, 245417 (2007); R. Roldan, J.-N. Fuchs, and M. O. Goerbig, Phys. Rev. B **80**, 085408 (2009); C. H. Yang, F. M. Peeters, and W. Xu, Phys. Rev. B **82**, 075401 (2010); P. K. Pyatkovskiy and V. P. Gusynin, Phys. Rev. B **83**, 075422 (2011).
[28] M. C. Bønsager, K. Flensberg, B. Y.-K. Hu, and A.-P. Jauho, Phys. Rev. Lett. **77**, 1366 (1996); Phys. Rev. B **56**, 10314 (1997).
[29] In strong magnetic fields, it is an intricate task to take into account the effect of screening properly covering a reasonably wide range of filling factors. The random phase approximation is commonly adopted [31,32] for the interlayer screened Coulomb potential $U(q,\omega,B)$ to capture the main features of screening under strong magnetic fields in which the fractional quantum Hall effect is not yet developed.
[30] See Supplemental Material at http://link.aps.org/supplemental/10.1103/PhysRevLett.122.186602 for details of the interlayer Coulomb interaction $U(q,\omega,B)$ in the statically screened random phase approximation. When compared to dynamical screening, we argue that the error in using the static screening approximation is not significant. Generally, the Thomas-Fermi screening assumption $\Pi(q,\omega,B) = \Pi(q=0,\omega=0,B)$ overestimates screening,

particularly at small q. This overestimation is suppressed by the q^2 dependence in the integrand of Eq. (8), which minimizes the contribution of the small q region in which the static screening assumption is most inaccurate. Furthermore, in our case with sharp LLs, static screening assumption also underestimates screening due to the neglect of $\mathrm{Im}\Pi(q,\omega,B)$ that becomes large at inter-LL transitions. The errors due the general overestimation of screening and the neglect of inter-LL transitions tend to cancel.

[31] I. V. Gornyi, A. D. Mirlin, and F. von Oppen, Phys. Rev. B **70**, 245302 (2004).

[32] A. V. Khaetskii and Y. V. Nazarov, Phys. Rev. B **59**, 7551 (1999).

[33] B. Y.-K. Hu, Phys. Scr. **1997**, 170 (1997).

[34] A similar mechanism for drag was proposed [35] in the context of the spin Hall effect. In double-layer systems with spin-orbit coupling and without a magnetic field, the presence of the intralayer spin Hall effect was shown to lead to a spin Hall drag resistivity.

[35] S. M. Badalyan and G. Vignale, Phys. Rev. Lett. **103**, 196601 (2009).

[36] C. R. Johnson, Am. Math. Mon. **77**, 259 (1970).

[37] While the interlayer energy drag mechanism [13,14] accounts for the negative drag resistivity at the simultaneous CNP observed under weak magnetic fields [16,17], it produces results that are opposite in sign to those observed in recent experiments conducted under a strong magnetic field [22]. It is therefore possible that the momentum exchange mechanism starts to dominate the energy exchange mechanism when the magnetic field becomes strong. Further experimental and theoretical work will be needed to clarify this point.

[38] M. Schutt, P. M. Ostrovsky, M. Titov, I. V. Gornyi, B. N. Narozhny, and A. D. Mirlin, Phys. Rev. Lett. **110**, 026601 (2013).